

Research Article

Towards a Reproducible Synthesis of High Aspect Ratio Gold Nanorods

Susanne Koeppel,¹ Christian Solenthaler,¹ Walter Caseri,² and Ralph Spolenak¹

¹Laboratory for Nanometallurgy, Department of Materials, ETH Zürich, 8093 Zürich, Switzerland

²Polymer Technology, Department of Materials, ETH Zürich, 8093 Zürich, Switzerland

Correspondence should be addressed to Walter Caseri, walter.caseri@mat.ethz.ch

Received 29 April 2010; Accepted 18 July 2010

Academic Editor: Quanqin Dai

Copyright © 2011 Susanne Koeppel et al. This is an open access article distributed under the Creative Commons Attribution License, which permits unrestricted use, distribution, and reproduction in any medium, provided the original work is properly cited.

The seed-mediated method in presence of high concentrations of CTAB is frequently implemented in the preparation of high aspect ratio gold nanorods (i.e., nanorods with aspect ratios of 5 or more); however, the reproducibility has still been limited. We rendered the synthesis procedure simpler, decreased the susceptibility to impurities, and improved the reproducibility of the product distribution. As a result of the high aspect ratios, longitudinal plasmon absorptions were shifted up to very high absorption maxima of 1955 nm in UV-vis-NIR spectra (since this band is completely covered in aqueous solution by the strong absorption of water, the gold species were embedded in poly(vinyl alcohol) films for UV-vis-NIR measurements). Finally, the directed particle growth in (110) direction leads to the conclusion that the adsorption of CTAB molecules at specific crystal faces accounts for nanorod growth and not cylindrical CTAB micelles, in agreement with other observations.

1. Introduction

The preparation of gold nanorods has found wide attention during the last decade since many characteristics of nanoscale materials are size- and shape-dependent including their optical, electronic, and catalytic properties. Spherical particles form readily in common synthesis methods for gold nanoparticles, but if the generation of spherical particles is suppressed by application of special conditions, besides rods [1, 2] also cubes [3–5], triangles [4, 6], and prisms [6] can arise. The synthesis of low aspect ratio nanorods, that is, nanorods with aspect ratios of 3 or less, has been reported in high yields [3, 4, 7–9] and can readily be reproduced (Figure 1). Yet the controlled and reproducible fabrication of high aspect ratio gold nanorods, that is, nanorods with an aspect ratio of 5 or more, by the most common method is still crucial. Therefore, fundamental aspects such as vis-NIR absorption spectra of high aspect ratio nanorods or their principal growth mechanism are still not connectedly investigated.

A number of synthesis methods for high aspect ratio rod-like nanocrystals have been described [1, 6, 10–14], such

as the template method [15, 16], electrochemical methods [2, 17], microwave rapid heating [18], and the seed-mediated growth method [10, 19, 20]. The last synthesis procedure, which was favorably introduced by Murphy and coworkers in 2001 [1], has found most attention so far. Indeed, this way is accessible with ubiquitous laboratory equipment and offers the possibility to prepare higher quantities of nanoparticles than with other methods [21]. However, it has been pointed out that the reproducibility of the results thus obtained is limited [3, 7], in line with our own experiences: the yield of the nanorods varies considerably—in some attempts high aspect ratio nanorods are almost completely absent, and those samples containing high aspect ratio nanorods contain areas with large fractions of spherical particles or low aspect ratio nanorods, and even large areas without high aspect ratio nanorods are present (Figure 2).

Many approaches have been undertaken to improve the original seed-mediated method, in particular by varying different parameters such as seed aging time [19], seed concentration or metal to seed ratio [4, 10, 19, 20], time intervals between the synthesis steps [10], pH value [10], additives [4, 5, 10, 11, 20], temperature [12], growth time

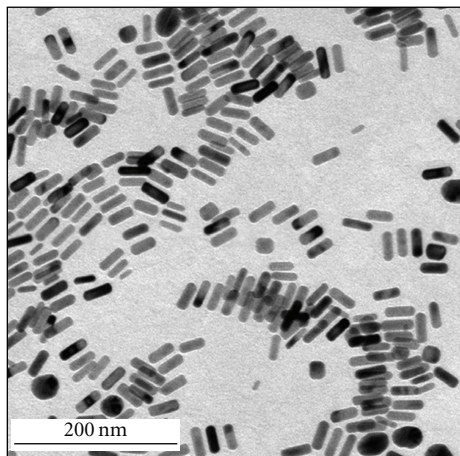


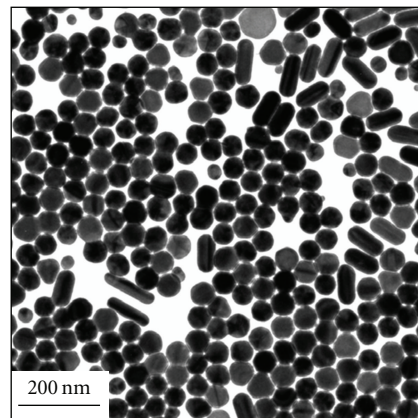
FIGURE 1: TEM image of an area with representative product distribution in samples containing low aspect ratio gold nanorods, prepared according to the seed-mediated method (in presence of small quantities of silver ions [3, 4, 7–9]). This image strongly resembles those reported elsewhere and shows that the synthesis of low aspect ratio gold nanorods is well reproducible (in contrast to high aspect ratio nanorods described so far).

[5], nature of the surfactant required for nanorod generation [6, 8], and the use of cosurfactants [5, 19]. In spite of this, the above addressed problems with respect to the creation of samples with high aspect ratio gold nanorods still persist.

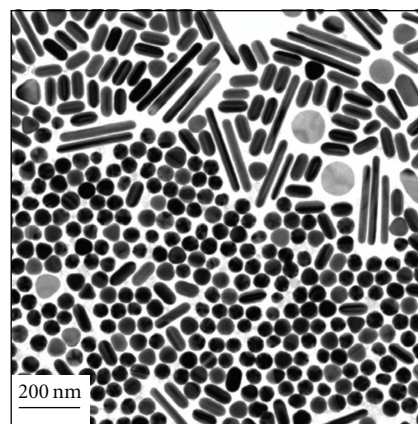
The limited reproducibility associated with the seed-methods described so far could be due to the relatively high number of the involved steps. In fact, we describe in the following that the reproducibility can be improved by the reduction of steps, which also renders the product formation less susceptible to impurities. Also, a simple method for the removal of excess surfactant required for the seed-mediated method was developed. The samples thus obtained were suited for the experimental determination of the position of the longitudinal plasmon absorption band of the gold rods in vis-NIR absorption spectra, which has been explored mainly with low aspect ratio nanorods so far [22–25], although also samples with high aspect ratio have been addressed [26, 27]. Further, the evaluation of electron diffraction patterns and other aspects provided information on the principal growth mechanism of the high aspect ratio nanorods.

2. Experimental

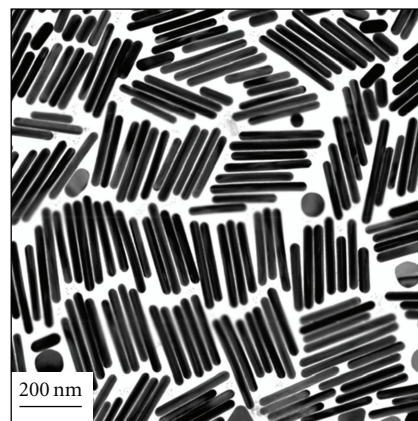
Hexadecyltrimethylammonium bromide (CTAB, designation H6269: 99%, or H5882: $\geq 98\%$, resp.) was purchased from Sigma or Fluka (CTAB, 96%), respectively. Hydrogen tetrachloroaurate trihydrate ($\text{H}[\text{AuCl}_4] \cdot 3\text{H}_2\text{O}$, 99.99%), hydrogen tetrachloroaurate hydrate ($\text{H}[\text{AuCl}_4] \cdot x\text{H}_2\text{O}$, 99.999%, x is not specified), hydrogen tetrachloroaurate ($\text{H}[\text{AuCl}_4]$, 100%), sodium tetrachloroaurate dihydrate ($\text{Na}[\text{AuCl}_4] \cdot 2\text{H}_2\text{O}$, 99.99%), and hydrogen tetrabromoaurate hydrate ($\text{H}[\text{AuBr}_4] \cdot x\text{H}_2\text{O}$, 99.99%, $x \approx 5$) were purchased from Alfa Aesar. Sodium citrate dihydrate (99%) was purchased from Sigma and sodium borohydride (NaBH_4)



(a)



(b)



(c)

FIGURE 2: TEM images of different spots of a sample containing high aspect ratio gold nanorods, prepared according to the seed-mediated method [1, 6, 10–14]. It is obvious that the nanorods are not evenly distributed over the TEM grids.

from Fisher Scientific (general purpose grade), Fluka (96%), or TCI ($>93\%$). L-ascorbic acid was obtained from Hanseler AG (Herisau, Switzerland). Titrisol ampoules were used for sodium hydroxide 0.1 M. All chemicals were used without further purification. For the preparation of all samples, freshly deionized water was used if not otherwise mentioned.

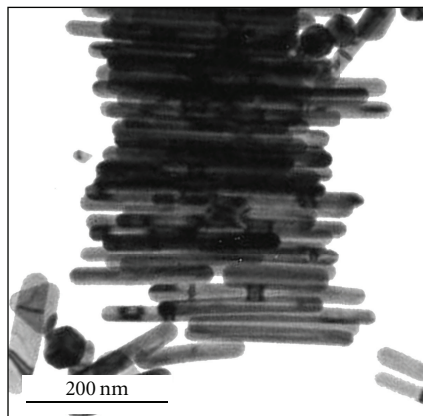


FIGURE 3: TEM image of a spot which is dominated by gold nanorods, prepared according to the “ordinary” synthetic conditions described in the Experimental section. As in the seed-mediated method, areas which do not contain essential fractions of particles other than nanorods can be found.

Poly(vinyl alcohol) (MW \approx 72000, Biochemica, where the type of MW has not been specified by the supplier) was purchased from Axon Lab (Applichem GmbH, Darmstadt, Germany).

2.1. Synthesis of Gold Nanorods. In a typical experiment, 2.5 mL of a 0.01 M $\text{H}[\text{AuCl}_4] \cdot 3\text{H}_2\text{O}$ solution and 3.6445 g hexadecyltrimethylammonium bromide (CTAB) were replenished to 100 mL in a volumetric glass flask. For completely dissolving the CTAB powder, it was necessary to keep this solution at elevated temperature (33°C) for at least 2 hours. This solution, which contained 0.1 M CTAB and $2.5 \cdot 10^{-4}$ M $\text{H}[\text{AuCl}_4] \cdot 3\text{H}_2\text{O}$, was used as *growth solution*.

During the dissolution of the CTAB in the above growth solution, a *seed solution* containing small gold particles was prepared as follows: a volume of 0.5 mL of 0.01 M $\text{H}[\text{AuCl}_4] \cdot 3\text{H}_2\text{O}$ solution ($5 \cdot 10^{-6}$ mol $\text{H}[\text{AuCl}_4] \cdot 3\text{H}_2\text{O}$, volumetric glass flask, not cooled) was added to 18.4 mL of ice-cooled deionized water in a wide-necked PE-flask (PE = polyethylene). Thereafter, 0.5 mL of freshly prepared 0.01 M sodium citrate solution ($5 \cdot 10^{-6}$ mol sodium citrate, solution in a volumetric glass flask, not cooled) was added. Thereafter, immediately 0.6 mL of freshly prepared 0.1 M NaBH_4 solution (in a glass vessel) cooled in an ice-bath was added, and the resulting solution was stirred for 30 s (there was no significant difference in the results whether the used pipettes were previously ice-cooled or not). The solution turned red (after 24 h, particles of a size of approximately 8 nm formed, as evident from transmission electron microscopy). Changing the sequence in the addition of substances in the seed preparation did not lead to significantly different results with respect to nanorod generation.

For the following final reaction steps, cooling was not required. 80 μL of a freshly prepared 0.1 M ascorbic acid solution ($8.0 \cdot 10^{-6}$ mol ascorbic acid) was added without stirring to 14.4 mL of the growth solution (age between 2 h and 24 h, containing $3.6 \cdot 10^{-6}$ mol gold). The solution was

mixed by shaking, whereupon the solution became colorless indicating the reduction of Au(III) to Au(I). In the next step, 80 μL of 0.1 M sodium hydroxide solution ($8.0 \cdot 10^{-6}$ mol NaOH) was added to the solution to modify the pH value. After addition of 16 μL of seed solution (age between 2 h and 24 h, containing $4.0 \cdot 10^{-9}$ mol gold), the solution was mixed by shaking and became reddish during this period. Then the test tubes were placed in a water bath at 33°C for 3 h–168 h and finally stored in a refrigerator (temperature \approx 6°C) to precipitate a major fraction of CTAB which could be removed by rapid filtration through a sintered glass funnel (pore size G4). The filtered samples were stable for at least 6 months in aqueous solution in the refrigerator or at room temperature. Probably, the dispersion was stabilized by residual surfactant.

2.2. Transmission Electron Microscopy. For investigations by transmission electron microscopy (TEM), either a Philips CM200 (160 kV accelerating voltage) or a Philips CM30 (300 kV accelerating voltage) was used. The average length, width, and aspect ratio of the nanorods were determined by counting several hundred particles with an aspect ratio bigger than 2 (manual evaluation of several TEM images). In order to obtain reliable images, a considerable part of the excess of CTAB had to be removed by filtration of the cold solution resulting from the synthesis (see above). Finally, one droplet ($\approx 0.5 \mu\text{L}$) of the filtered solution was put on a commercially available carbon-coated copper TEM grid (Plano GmbH, Wetzlar, Germany).

2.3. Scanning Electron Microscopy. For investigation with scanning electron microscopy (SEM), a Zeiss NVision 40 was used. For sample preparation, cold solutions were filtered to remove CTAB, then centrifuged at 5600 rpm for 10 min followed by decantation to remove another part of the excess of CTAB, and finally the remaining solids were dissolved in water. One droplet ($\approx 0.5 \mu\text{L}$) of this solution was put on a pyrolytic graphite (spi supplies, West Chester, PA, USA).

2.4. UV-vis-NIR Spectra. UV-vis-NIR absorption spectra were performed with a Lambda 900, Perkin Elmer, Überlingen, Germany.

In order to detect the longitudinal absorption band of the gold nanoparticles, 53.5 mg poly(vinyl alcohol) (PVAL) were dissolved in 5 mL deionized water by heating to 90°C under stirring. After dissolution of the polymer, the solution was allowed to cool down to room temperature. Under vigorous stirring, 10 mL of a filtered gold particle solution was added to the PVAL solution at room temperature. The homogeneous mixture was poured in a flat aluminum dish, and the solvent was evaporated overnight at ambient conditions.

3. Results and Discussion

3.1. General Procedure of Nanorod Generation. The seed-mediated method is based on anisotropic particle growth

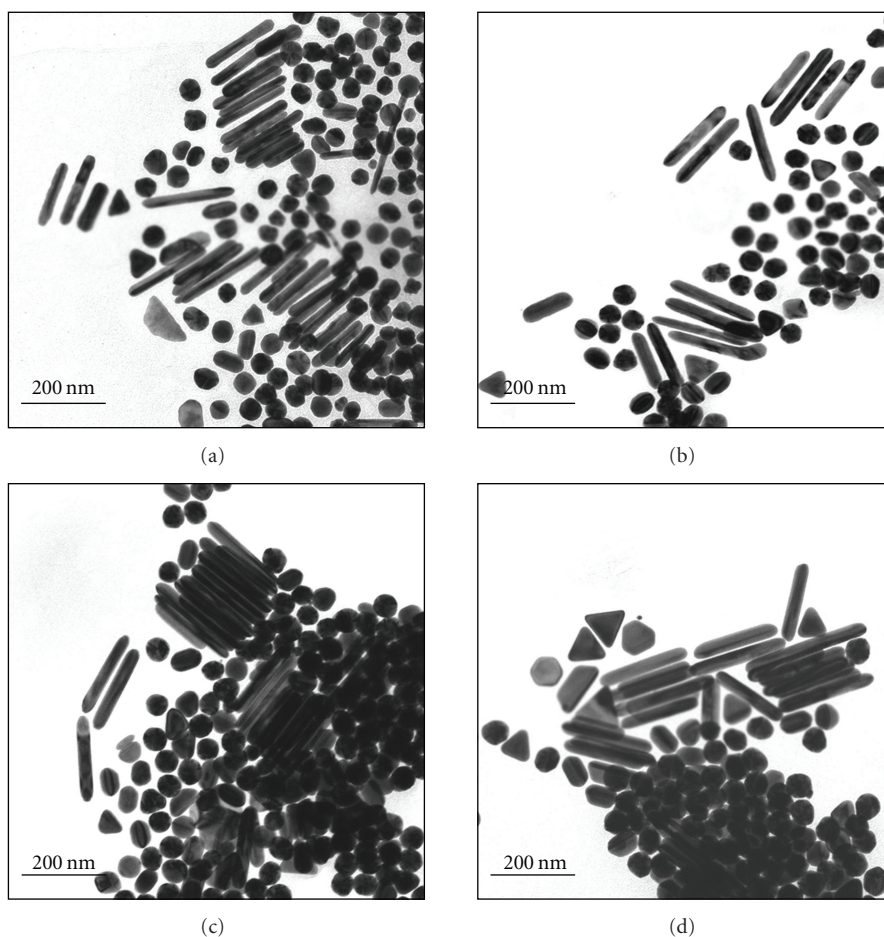


FIGURE 4: TEM images of different samples ((a)–(d)) of gold nanorods. The images illustrate representative ratios between rods and other particles.

by combining a so-called seed solution comprising spherical gold nanoparticles with a growth solution containing tetrachloroaurate(III) and a surfactant. Commonly CTAB (cetyltrimethylammonium bromide, hexadecyltrimethylammonium bromide) is used for this purpose, in presence of a reducing agent, and the resulting solution is subsequently further processed. A main difference between the synthesis procedure described here and the methods reported previously (see Introduction) is keeping additives and processing steps at a minimum. In particular, additives such as silver ions or surfactants in the seed solution, repeated steps of dilution and addition of growth solution, or extended centrifugation procedures of the final solutions are not required anymore. Essential particularities of the seed-mediated method created here are rapid addition of a small volume of seed solution (on the order of $10\ \mu\text{L}$) in the final step of the synthesis procedure and modification of the pH value by a defined quantity of sodium hydroxide. In numerous preliminary experiments, parameters such as growth time, age of the seed and growth solution, and growth temperature were varied which finally resulted in the propitious conditions described in the Experimental section.

The recipe in the Experimental section provided nanorods of aspect ratios around 6 in the average and 10

or more at maximum. When investigating the samples with transmission electron microscopy (TEM), it was possible to find places which showed almost exclusively nanorods (Figure 3); however, significant quantities of spherical and, to a lesser extent, triangular particles also arose, in line with other publications on seed-mediated growth of high aspect ratio gold nanorods [1, 6, 10, 12, 14, 28] and own experiments performed according to previously reported syntheses (Figure 2). It has been reported that spheres and platelets can be substantially removed by sedimentation followed by chemical treatments [27]; however, it was clearly evident from TEM micrographs of products of our experiments that the aspect ratios markedly decreased by this procedure. Representative TEM images of four batches prepared at different days with different starting solutions and by two different persons (samples (a)–(d)) are shown in Figure 4. These samples contain nanorods of similar lengths (Figure 5), widths (Figure 6), and aspect ratios (Figure 7). Further, numerous spherical particles of typically 30 nm–60 nm and particles of other shapes (roughly 1/4 of the number of spherical particles) emerged. The samples' features were similar at reaction times (starting at the combination of growth and seed solution) of 3 h, 24 h, and 168 h, that is, nanorod formation was essentially established within 3 h.

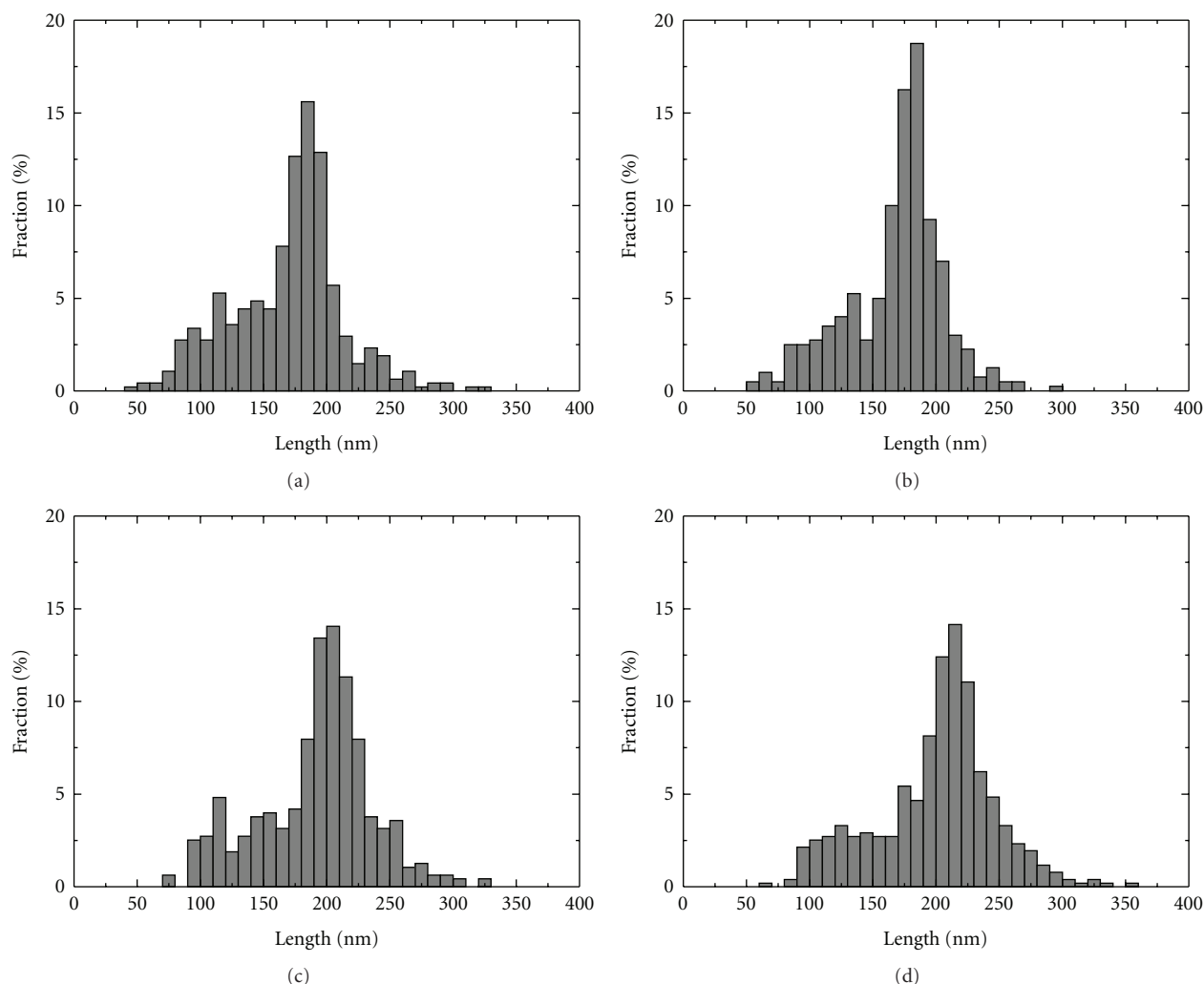


FIGURE 5: Length distributions of the rods corresponding to samples (a)–(d) of Figure 4.

Scanning electron microscopy (SEM) disclosed that the nanorods were not cylindrical but exhibited crystallographic facets (Figure 8).

For some applications, as for instance for investigations of the gold species by TEM, the large excess of CTAB needs to be removed. Thus, a major fraction of CTAB was simply precipitated by storage of the samples at ca. 6°C during 24 h and subsequent filtration. The gold nanorods in such filtrates were stable for at least a few months at room temperature or in the refrigerator. Separation of the CTAB by centrifugation/decantation cycles [1, 3, 4, 6, 7, 9–14, 19, 20, 28, 29] was more laborious and frequently led to the formation of gold particle agglomerates which did not redisperse readily in water.

An additional advantage of the presented synthesis method is the tolerance towards impurities which have otherwise reported to influence the yield, shape, and size of the gold particles. For instance, it was emphasized that ultra-pure water should be employed for nanorod formation by seed-mediated methods [3–10, 12, 19, 24, 28]. We found a minor influence of the water quality; however, surprisingly

the use of common freshly deionized water leads to better reproducibility than ultra-pure water. Maybe the ultra-pure water contained less but more critical impurities than the deionized water. As a consequence, all results reported here refer to experiments with deionized water. Further, impurities (in particular iodide) in the CTAB which depend on the suppliers [9] and the growth temperature [13, 28] have been reported to influence the rod formation. In particular, the commercial products H5882 and H6269 from Sigma and the CTAB from Fluka were reported to lead to strikingly different results in other seed-mediated methods [9]. However, the nanorod formation did not depend considerably on those CTAB qualities in the method presented here. Also, the nature of the gold salt ($\text{H}[\text{AuCl}_4]$, $\text{H}[\text{AuCl}_4] \cdot x\text{H}_2\text{O}$ where x is not specified, $\text{H}[\text{AuCl}_4] \cdot 3\text{H}_2\text{O}$, $\text{H}[\text{AuBr}_4] \cdot x\text{H}_2\text{O}$ with $x \approx 5$, and $\text{Na}[\text{AuCl}_4] \cdot 2\text{H}_2\text{O}$) had a minor influence on product formation.

Variation of reaction parameters did not improve the creation of high aspect ratio nanorods over all. When the pH value was varied between 3.4 and 10.1 (compared to 3.9 at “ordinary” conditions) with NaOH, the nanorod generation

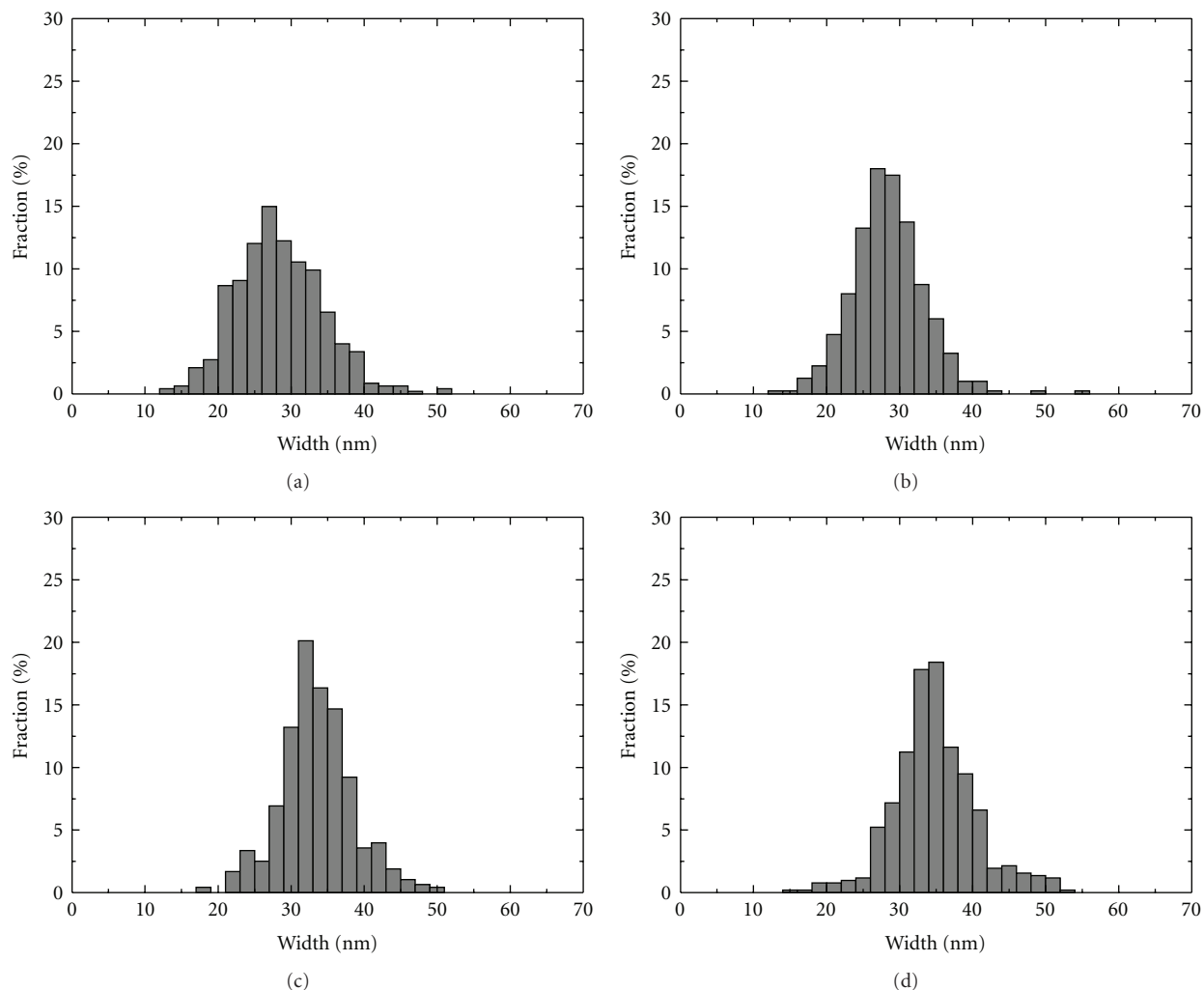


FIGURE 6: Width distributions of the rods corresponding to samples (a)–(d) of Figure 4.

was pronouncedly influenced (Figure 9), as also observed for other seed-mediated methods [10]. A low pH value (3.4) induced the formation of long nanorods, as also found in other seed-mediated procedures [26, 30], with a length on the order of 400 nm and a width between 15 and 20 nm, but the yield of these rods was very low and the aspect ratio distribution was relatively broad. Above a pH value of 6.6 or more, no rods arose anymore.

In the literature, an increase in seed particle concentration resulted in a decrease of the aspect ratio [19, 20]; however, the concentrations of the seeds were typically higher than in our experiments and we could not find a noteworthy improvement in aspect ratio when the concentration of the seed particles (age 24 hours, average diameter ≈ 8 nm) was varied between 0 and $3.77 \cdot 10^{-7}$ M (the concentrations refer to gold atoms in the final solutions). Yet the experiments showed clearly that the addition of seeds is necessary to grow rod-shaped particles as otherwise only spherical or irregularly shaped particles emerged.

When the concentration of the tetrachloroauric acid in the growth solution was varied, the molar ratio ascorbic

acid/sodium hydroxide/tetrachloroaurate(III) was kept constant. An increase in the tetrachloroaurate(III) concentration by a factor of 2 or 3 lead to an increase in aspect ratio of the nanorods (typically to 8 and 12, resp.), which was, however, accompanied by an increase in polydispersity (Figure 10). Yet when the tetrachloroaurate(III) concentration was increased by a factor of 6, the nanorods became thicker and shorter, that is, the aspect ratio decreased to typical values of 4–5, and larger particles, such as triangles and spheres, also emerged in higher quantities.

Finally, we attempted to separate the gold nanorods from other particles according to the depletion-induced shape and size selection method [31]; however, we could not significantly enhance the fraction of nanorods in the samples.

3.2. Influence of the CTAB Concentration and Growth Mechanism. As far as we are aware of, it has not been pointed out in the context of seed-mediated nanorod formation that the phase diagram of CTAB [32] exhibits a triple point around a concentration of 0.1 M and a temperature around 25°C where crystals, individually dissolved molecules, and

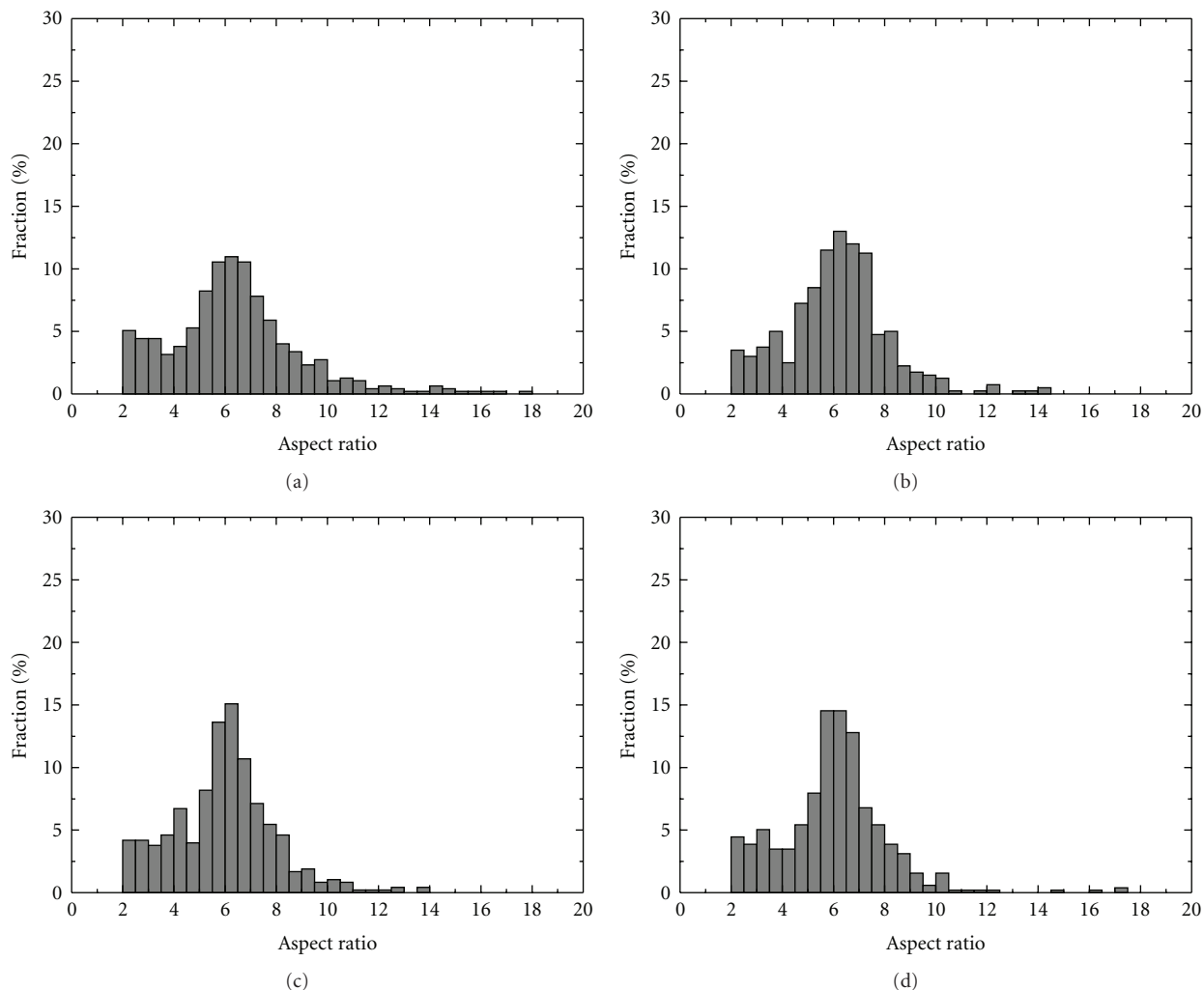


FIGURE 7: Aspect ratio distributions of the rods corresponding to samples (a)–(d) of Figure 4.

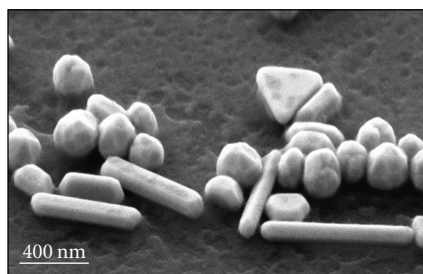


FIGURE 8: SEM image of gold nanorods and other species, taken at a tilt angle of 54° .

spherical micelles coexist. Accordingly, we kept the solutions containing 0.1 M CTAB at 33°C (enhancement of the temperature to 50°C did not alter the nanorod formation noteworthy, in contrast to other seed-mediated procedures [13, 28]) in order to avoid precipitation of CTAB which indeed slowly occurred in 0.1 M solutions close to 25°C .

Since CTAB is essential for nanorod formation, the CTAB concentration in the growth solution, which is 0.1 M if not otherwise mentioned as common in other seed-mediated methods, was also decreased to 0.01 M or increased to 0.25 and 0.5 M, respectively. It was reported in other seed-mediated methods that at a CTAB concentration of 0.01 M higher aspect ratios result when the synthesis is performed at 0°C [13]; we note, however, that CTAB precipitates under these conditions by our experience, in agreement with the above-mentioned phase diagram. At a concentration of 0.01 M of CTAB at 33°C , only spherical particles and egg-like shaped particles arose (Figure 11), while an increase in the CTAB concentration from 0.1 M to 0.25 M did not lead to a significant change of aspect ratio and yield of gold nanorods. However, at a CTAB concentration of 0.5 M, only a few very big spherical particles and triangles emerged (Figure 11). These findings are different from those of other seed-mediated methods where the yield of high aspect ratio nanorods increased with decreasing CTAB concentration [13], while, in contrast, other authors report that the aspect ratio increases with higher CTAB concentrations [26].

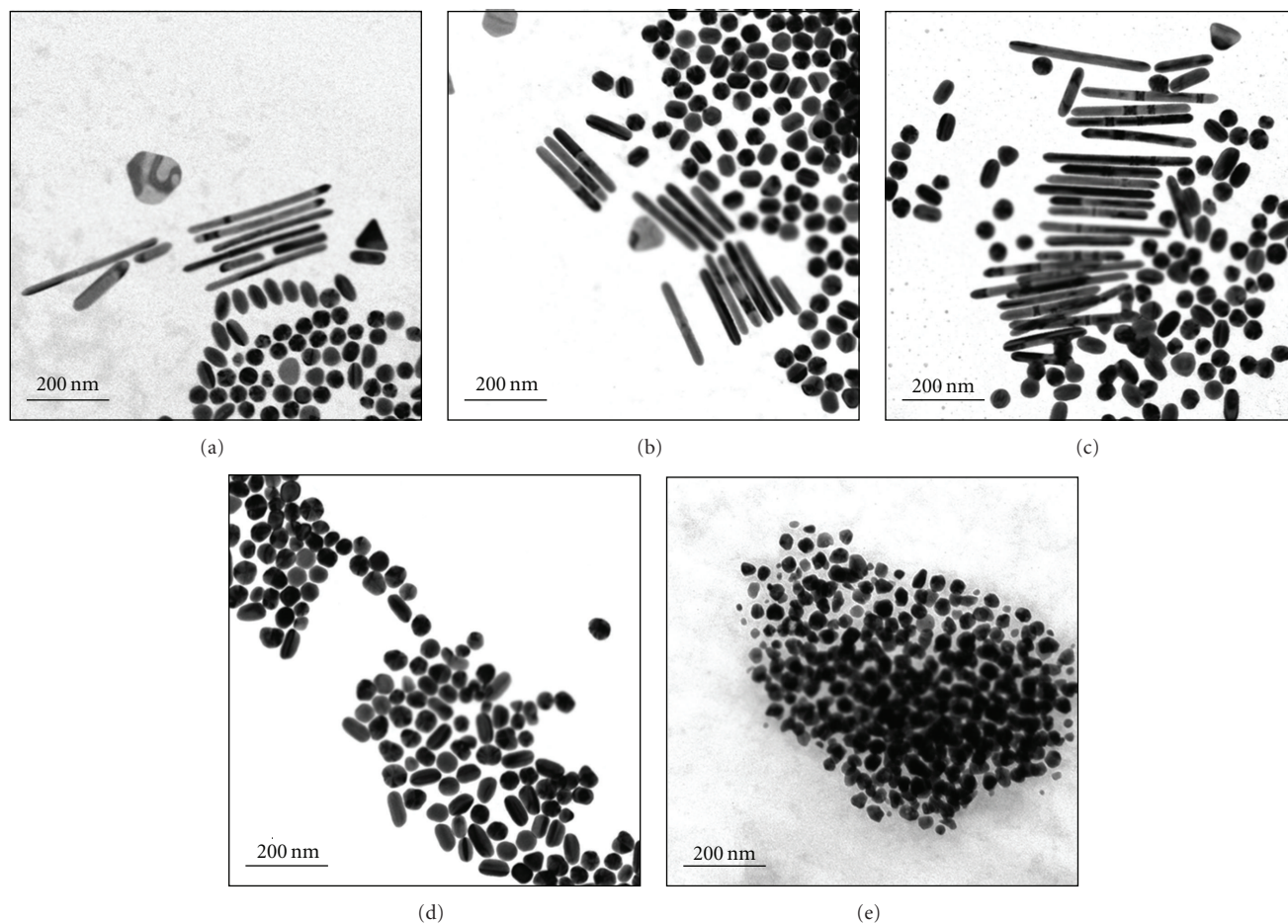


FIGURE 9: TEM images of gold nanorods prepared at pH values of 3.4 (a), 3.9 (b), 5.9 (c), 6.6 (d) and, 10.1 (e).

Of course, the CTAB concentration is associated with the growth mechanism of the nanorods. A growth mechanism which has been discussed in the literature is based on the ability of CTAB to form micelles [1]. Accordingly it was proposed that the gold particles grow inside these micelles and their shape is therefore determined by the shape of the micelles which depends on the concentration of the surfactant. However, with regard to the above mentioned phase diagram of CTAB, spherical and not cylindrical micelles are expected at the conditions commonly applied in seed-mediated methods (0.1 M CTAB), and only at higher concentration (above around 0.3 M), cylindrical micelles arise [32]; yet our experiments with 0.5 M CTAB did not yield nanorods. Therefore, we consider the formation of nanorods within CTAB micelles not to be likely. In this context, it is also worth to note that the nanorods' shapes are not cylindrical (see Figure 8).

As an alternative explanation for nanorod formation, the CTAB molecules could adsorb preferentially to certain crystal faces and therewith inhibit isotropic crystal growth, thus producing the shape of a rod [13]. This mechanism would explain at least that rod formation did not occur at low CTAB concentrations (0.01 M) assuming that the equilibrium constant is in these cases too low for an effective

adsorption of CTAB at the crystal faces. On the other hand, at the highest concentration applied here (0.5 M), for instance, the formation of cylindrical micelles might compete with CTAB adsorption at the gold crystal faces, that is, less CTAB molecules might be available for adsorption at gold particles which then could lead to isotropic particle growth, that is, formation of spherical particles. Importantly, electron diffraction patterns (Figure 12) identified the (110) direction as the growth direction. This indeed implies that the nanorod growth is associated with adsorption of CTAB molecules at specific crystal faces as otherwise a random growth direction of the rods is expected.

3.3. UV-vis-NIR Absorption Spectra. Extensive UV-vis-NIR studies have been performed previously with low aspect ratio gold nanorods [22–25, 29], and corresponding measurements were only performed for wavelengths ranging from 300 nm to 1300 nm. Basically, gold nanorods give rise to two absorption bands. One of them is caused by transverse oscillations of the electrons (transverse absorption band), which is typically located in the visible wavelength region, and one due to the longitudinal oscillations of the electrons (longitudinal absorption band) [33]. The longitudinal

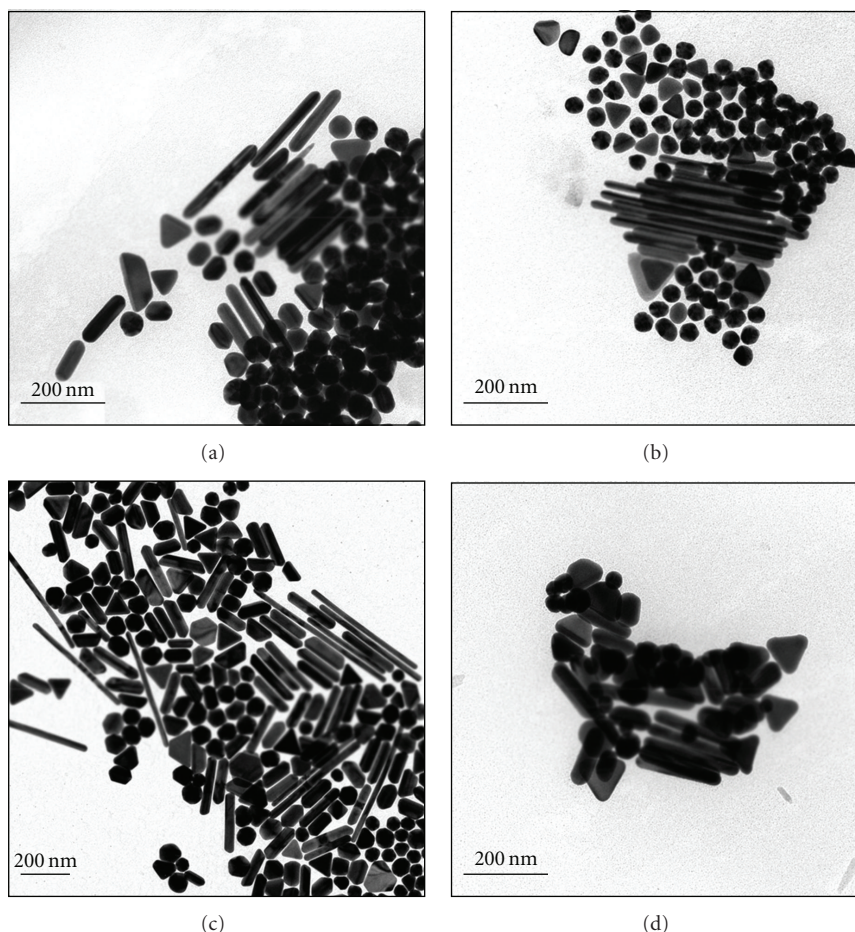


FIGURE 10: TEM images of gold nanorods prepared with different concentrations of tetrachloroauric acid in the growth solution: $2.5 \cdot 10^{-4}$ M (a), $5 \cdot 10^{-4}$ M (b), $7.5 \cdot 10^{-4}$ M (c), and $1.5 \cdot 10^{-3}$ M (d).

absorption band is shifted from the visible towards the near-infrared region with increasing aspect ratio, whereas the transverse band can interfere with the absorption of spherical gold particles.

Remarkably, reliable experimental information on the longitudinal band for high aspect ratio gold nanorods is rarely available so far. Indeed, the longitudinal absorption band of such particles in UV-vis-NIR spectra falls in the absorption region of water (ca. 1300 nm–above 2500 nm) and is therefore not accessible in the aqueous solutions finally resulting from the nanorod synthesis (subtraction of the water absorption band does not lead to reliable results due to the very high (“infinite”) absorbance at common experimental setups). Therefore, we used a technique which bases on embedding the particles in poly(vinyl alcohol) (PVAL), which is water-soluble, does not absorb pronouncedly in the UV-vis-NIR region, and readily forms transparent free-standing composite films with gold by solution casting (see Experimental part). In order to investigate if the residual water content in PVAL influences the UV-vis-NIR spectra of the gold particles, a PVAL film with and without gold, respectively, was measured after drying the film at ambient conditions for 3 days at room temperature, subsequently

a second spectrum after drying under vacuum (ca. 1 mbar) for one day, and finally a third spectrum after storing the dried PVAL film in an atmosphere with humidity of ca. 99% for 18 days was recorded. The three spectra are shown in Figure 13, after subtraction of the spectrum of analogously treated blank PVAL films (the absorbance of which, however, was only marginal). It is obvious that the two absorption maxima at 520 nm and around 1955 nm (broad) are independent of the water content (minor differences may occur because the exact position of the sample in the spectrometer is not identical in the three spectra). A less pronounced absorption maximum or shoulder around 675 nm varies to a certain extent in relative intensity, which might be due to swelling effects [34]. The peaks in the region of 500–700 nm are attributed to the more or less spherical particles, triangles and the transversal plasmon absorption of the nanorods and that around 1955 nm to the longitudinal absorption of the nanorods. This band is shifted markedly to higher wavelengths compared to that of particles reported with lower aspect ratio (520 nm–1000 nm [23, 25]). Therefore, the UV-vis-NIR spectra confirm that a significant fraction of gold nanorods with relatively high aspect ratio is present in the sample.

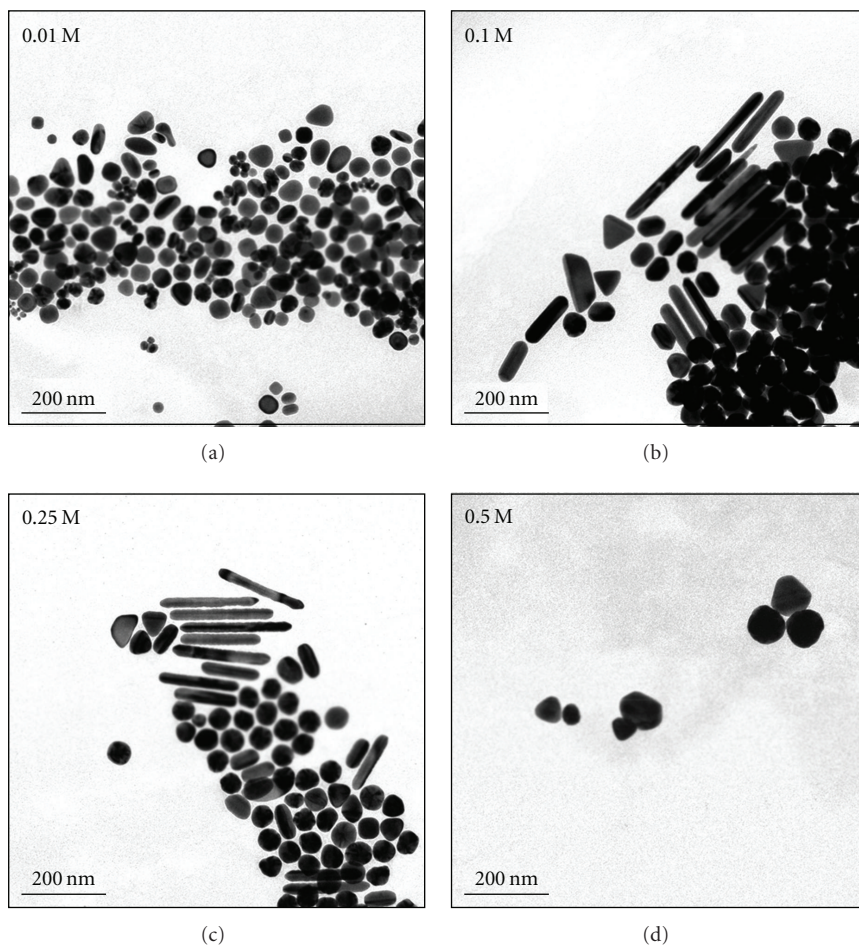


FIGURE 11: TEM images of gold nanorods prepared with different concentrations of CTAB; that is, 0.01 M, 0.1 M, 0.25 M, and 0.5 M.

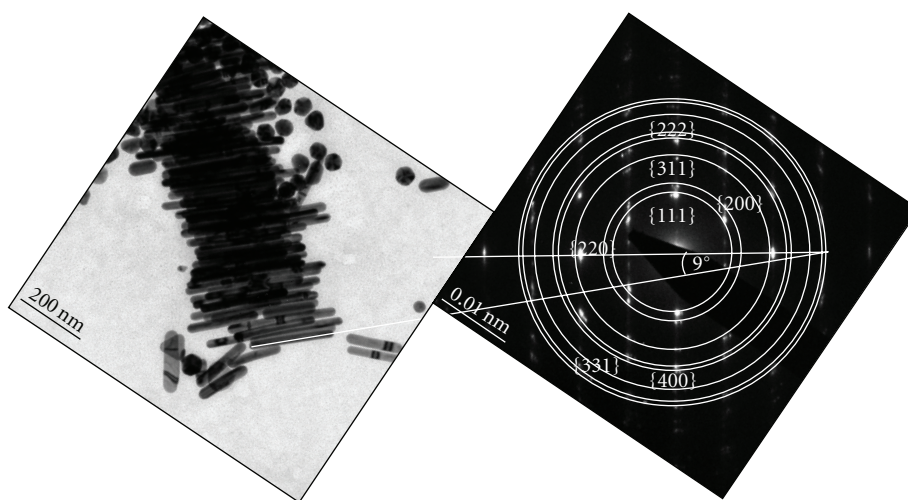


FIGURE 12: TEM image and related electron diffraction pattern used for the evaluation of the growth direction of the nanorods. The angle of 9° corresponds to the instrumental rotation of the diffraction pattern towards the bright field image at the employed magnification and camera length.

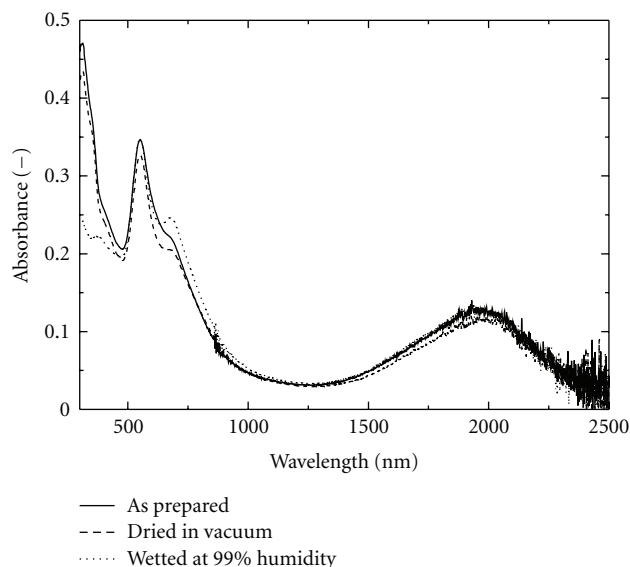


FIGURE 13: UV-vis-NIR spectra of gold particles (prepared according to the “ordinary” synthetic conditions described in the Experimental section) embedded in poly(vinyl alcohol) at different drying states after background subtraction.

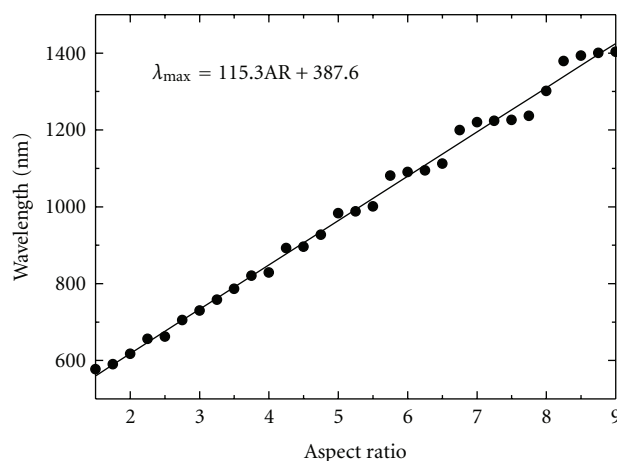


FIGURE 14: Calculated correlation between aspect ratio of gold nanoparticles embedded in poly(vinyl alcohol) and the absorption maximum of the longitudinal absorption band.

A linear correlation between the absorption maximum of the aspect ratio and the longitudinal absorption band was reported on the basis of Gans’ extension of Mie’s theory [33, 35]. However, the calculations referred to aqueous solutions which exhibit dielectric constants that clearly differ from those of poly(vinyl alcohol). Hence, we used the Gans formula for the recalculation of the aspect ratio-absorption maximum correlation with a dielectric constant for poly(vinyl alcohol) of 2.28 (average of indicated values for this polymer [2.2201–2.3409], calculated from the refractive index [36]), which resulted in the formula

$$\lambda_{\max} = 115.3AR + 387.6 \quad (1)$$

as derived from Figure 14 obtained by fitting of the wavelength of the longitudinal absorption maximum as a function of the aspect ratio (AR). Accordingly, the experimentally found absorption maximum of 1955 nm corresponds to an aspect ratio of 13.6 which is somewhat higher but still reasonably close to the average aspect ratios of the considered sample which may contribute to the respective absorption (obtained from TEM images, Figure 15). Deviations between theoretical and experimental values could be a consequence of, for example, the limited precision of the dielectric constant of poly(vinyl alcohol) (a range of dielectric constants is reported), the limited precision in the determination of the absorption maximum due to the broadness of the peak, the limited number of nanorods that can be evaluated by TEM compared to the total number of nanorods in the system, the presence of cylindrical instead of ellipsoidal shapes (the latter being the basis of Gans’ theory), or limits in the availability of the applied formula. The high value of 1955 nm is in the range of that of gold nanorod samples prepared by Wei et al. (1635 nm in D₂O) [26] and Khanal et al. (1567 in D₂O) [27].

4. Summary

An improvement in reproducibility of the gold species with high aspect ratio was achieved by reducing the steps in the seed-mediated growth method in presence of high concentrations of CTAB, which is based on the rapid addition of a small volume of seed particles (on the order of 10 μL). A major part of the CTAB could be removed after synthesis simply by precipitation at 6°C followed by filtration. Further, the synthesis route is less susceptible to impurities in the water or in the CTAB than indicated in other reports on the seed-mediated growth of gold nanorods. Nanorods with lengths on the order of 200 nm and aspect ratios around 6 in the average and 10 or more at maximum formed in significant amounts (the higher values, however, were accompanied by an increase in polydispersity), which was confirmed by UV-vis-NIR measurements, where the longitudinal plasmon absorption could readily be detected when the gold particles were embedded in poly(vinyl alcohol). Thus, maximum absorptions of nanoparticles with high aspect ratios were found at the extraordinarily high wavelength of 1955 nm. As evident from SEM, the rods were not cylindrical but exhibited crystallographic facets. Considering this fact, the phase diagram of CTAB and in particular electron diffraction patterns of the nanorods, nanorod formation appears to be induced rather by preferential CTAB adsorption at specific faces of the growing crystals than by particle growth in the interior of cylindrical CTAB micelles.

Acknowledgments

The authors thank Pascal Wolfer for synthesizing a badge of gold nanoparticles, Michael Roth, Barbara Grant, Anita Bardill, and Daniel Schmid for experimental help in our initial attempts, Stephan Frank for providing the MatLab routine for size evaluation, and Giancarlo Pigozzi for acquiring the diffraction patterns, support by the electron

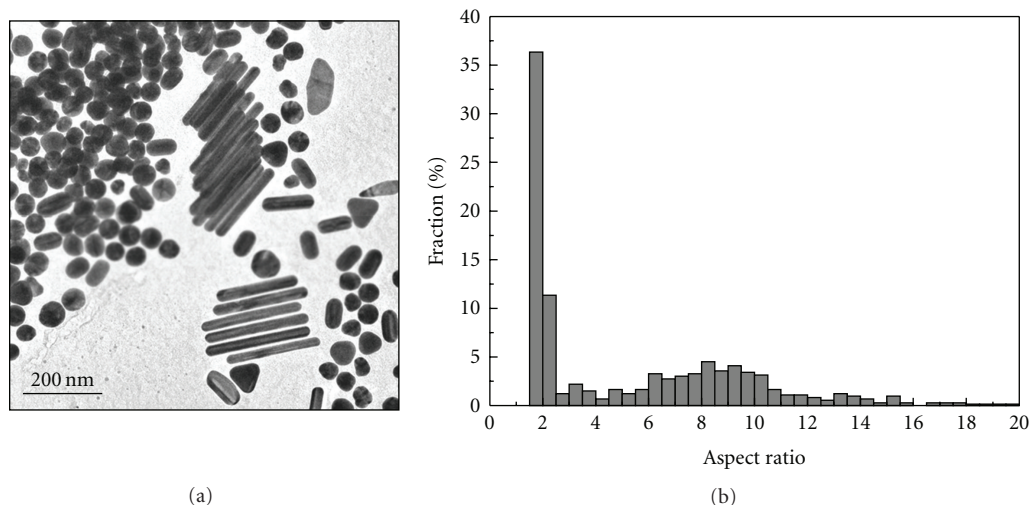


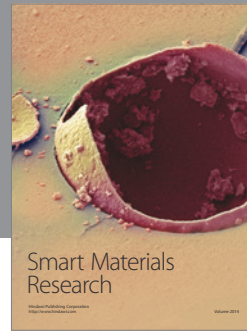
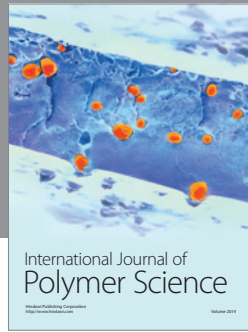
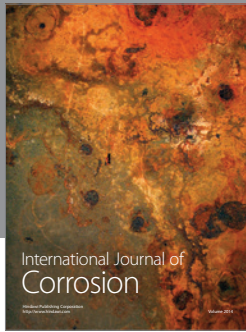
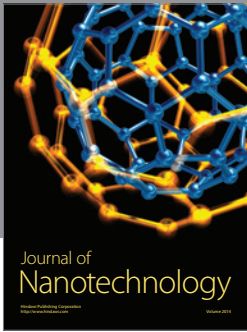
FIGURE 15: TEM image and aspect ratio distribution of the gold nanorods of the sample shown in Figure 13, which substantiate that indeed the absorption in the NIR region is associated with a high aspect ratio of gold nanorods.

microscopy center (EMEZ) of ETH Zurich and the Swiss National Science Foundation (SNF) for financial support under Project no. 200021-113463.

References

- [1] N. R. Jana, L. Gearheart, and C. J. Murphy, "Wet chemical synthesis of high aspect ratio cylindrical gold nanorods," *Journal of Physical Chemistry B*, vol. 105, no. 19, pp. 4065–4067, 2001.
- [2] Y. Yu, S. Chang, C. Lee, and C. R. C. Wang, "Gold nanorods: electrochemical synthesis and optical properties," *Journal of Physical Chemistry B*, vol. 101, no. 34, pp. 6661–6664, 1997.
- [3] X. C. Jiang and M. P. Pileni, "Gold nanorods: influence of various parameters as seeds, solvent, surfactant on shape control," *Colloids and Surfaces A*, vol. 295, no. 1–3, pp. 228–232, 2007.
- [4] T. K. Sau and C. J. Murphy, "Seeded high yield synthesis of short Au nanorods in aqueous solution," *Langmuir*, vol. 20, no. 15, pp. 6414–6420, 2004.
- [5] B. Nikoobakht and M. A. El-Sayed, "Preparation and growth mechanism of gold nanorods (NRs) using seed-mediated growth method," *Chemistry of Materials*, vol. 15, no. 10, pp. 1957–1962, 2003.
- [6] J. Gao, C. M. Bender, and C. J. Murphy, "Dependence of the gold nanorod aspect ratio on the nature of the directing surfactant in aqueous solution," *Langmuir*, vol. 19, no. 21, pp. 9065–9070, 2003.
- [7] X. C. Jiang, A. Brioude, and M. P. Pileni, "Gold nanorods: limitations on their synthesis and optical properties," *Colloids and Surfaces A*, vol. 277, no. 1–3, pp. 201–206, 2006.
- [8] D. K. Smith and B. A. Korgel, "The importance of the CTAB surfactant on the colloidal seed-mediated synthesis of gold nanorods," *Langmuir*, vol. 24, no. 3, pp. 644–649, 2008.
- [9] D. K. Smith, N. R. Miller, and B. A. Korgel, "Iodide in CTAB prevents gold nanorod formation," *Langmuir*, vol. 25, no. 16, pp. 9518–9524, 2009.
- [10] B. D. Busbee, S. O. Obare, and C. J. Murphy, "An improved synthesis of high-aspect-ratio gold nanorods," *Advanced Materials*, vol. 15, no. 5, pp. 414–416, 2003.
- [11] H.-Y. Wu, W.-L. Huang, and M. H. Huang, "Direct high-yield synthesis of high aspect ratio gold nanorods," *Crystal Growth and Design*, vol. 7, no. 4, pp. 831–835, 2007.
- [12] H. J. Park, C. S. Ah, W.-J. Kim, I. S. Choi, K.-P. Lee, and W. S. Yun, "Temperature-induced control of aspect ratio of gold nanorods," *Journal of Vacuum Science and Technology A*, vol. 24, no. 4, pp. 1323–1326, 2006.
- [13] S. K. Kang, S. Chah, C. Y. Yun, and J. Yi, "Aspect ratio controlled synthesis of gold nanorods," *Korean Journal of Chemical Engineering*, vol. 20, no. 6, pp. 1145–1148, 2003.
- [14] A. Gole and C. J. Murphy, "Seed-mediated synthesis of gold nanorods: role of the size and nature of the seed," *Chemistry of Materials*, vol. 16, no. 19, pp. 3633–3640, 2004.
- [15] M. Wirtz, S. Yu, and C. R. Martin, "Template synthesized gold nanotube membranes for chemical separations and sensing," *Analyst*, vol. 127, no. 7, pp. 871–879, 2002.
- [16] C. R. Martin, "Membrane-based synthesis of nanomaterials," *Chemistry of Materials*, vol. 8, no. 8, pp. 1739–1746, 1996.
- [17] S.-S. Chang, C.-W. Shih, C.-D. Chen, W.-C. Lai, and C. R. C. Wang, "The shape transition of gold nanorods," *Langmuir*, vol. 15, no. 3, pp. 701–709, 1999.
- [18] F.-K. Liu, Y.-C. Chang, F.-H. Ko, and T.-C. Chu, "Microwave rapid heating for the synthesis of gold nanorods," *Materials Letters*, vol. 58, no. 3–4, pp. 373–377, 2004.
- [19] J. Pérez-Juste, L. M. Liz-Marzán, S. Carnie, D. Y. C. Chan, and P. Mulvaney, "Electric-field-directed growth of gold nanorods in aqueous surfactant solutions," *Advanced Functional Materials*, vol. 14, no. 6, pp. 571–579, 2004.
- [20] N. R. Jana, L. Gearheart, and C. J. Murphy, "Evidence for seed-mediated nucleation in the chemical reduction of gold salts to gold nanoparticles," *Chemistry of Materials*, vol. 13, no. 7, pp. 2313–2322, 2001.
- [21] J. Pérez-Juste, I. Pastoriza-Santos, L. M. Liz-Marzán, and P. Mulvaney, "Gold nanorods: synthesis, characterization and applications," *Coordination Chemistry Reviews*, vol. 249, no. 17–18, pp. 1870–1901, 2005.
- [22] B. M. I. Van Der Zande, L. Pagès, R. A. M. Hikmet, and A. Van Blaaderen, "Optical properties of aligned rod-shaped gold particles dispersed in poly(vinyl alcohol) films," *Journal of Physical Chemistry B*, vol. 103, no. 28, pp. 5761–5767, 1999.

- [23] S. Eustis and M. El-Sayed, "Aspect ratio dependence of the enhanced fluorescence intensity of gold nanorods: experimental and simulation study," *Journal of Physical Chemistry B*, vol. 109, no. 34, pp. 16350–16356, 2005.
- [24] J. Pérez-Juste, B. Rodríguez-González, P. Mulvaney, and L. M. Liz-Marzán, "Optical control and patterning of gold-nanorod-poly(vinyl alcohol) nanocomposite films," *Advanced Functional Materials*, vol. 15, no. 7, pp. 1065–1071, 2005.
- [25] S. Eustis and M. A. El-Sayed, "Determination of the aspect ratio statistical distribution of gold nanorods in solution from a theoretical fit of the observed inhomogeneously broadened longitudinal plasmon resonance absorption spectrum," *Journal of Applied Physics*, vol. 100, no. 4, Article ID 044324, 2006.
- [26] Q. Wei, A. Ji, and J. Shen, "PH controlled synthesis of high aspect-ratio gold nanorods," *Journal of Nanoscience and Nanotechnology*, vol. 8, no. 11, pp. 5708–5714, 2008.
- [27] B. P. Khanal and E. R. Zubarev, "Purification of high aspect ratio gold nanorods: complete removal of platelets," *Journal of the American Chemical Society*, vol. 130, no. 38, pp. 12634–12635, 2008.
- [28] S. K. Kang, Y. Kim, M. S. Hahn, I. Choi, J. Lee, and J. Yi, "Aspect ratio control of Au nanorods via temperature and hydroxylamine concentration of reaction medium," *Current Applied Physics*, vol. 6, no. 1, pp. e114–e120, 2006.
- [29] C. J. Murphy and C. J. Orendorff, "Alignment of gold nanorods in polymer composites and on polymer surfaces," *Advanced Materials*, vol. 17, no. 18, pp. 2173–2177, 2005.
- [30] F. Kim, K. Sohn, J. Wu, and J. Huang, "Chemical synthesis of gold nanowires in acidic solutions," *Journal of the American Chemical Society*, vol. 130, no. 44, pp. 14442–14443, 2008.
- [31] K. Park, H. Koerner, and R. A. Vaia, "Depletion-induced shape and size selection of gold nanoparticles," *Nano Letters*, vol. 10, no. 4, pp. 1433–1439, 2010.
- [32] N. K. Raman, M. T. Anderson, and C. J. Brinker, "Template-based approaches to the preparation of amorphous, nanoporous silicas," *Chemistry of Materials*, vol. 8, no. 8, pp. 1682–1701, 1996.
- [33] R. Gans, "Über die Form ultramikroskopischer Goldteilchen," *Annalen der Physik*, vol. 342, pp. 881–900, 1912, *Drude's Ann.* Vol. 37, pp. 881–900, 1912.
- [34] D. I. Uhlenhaut, P. Smith, and W. Caseri, "Color switching in gold—polysiloxane elastomeric nanocomposites," *Advanced Materials*, vol. 18, no. 13, pp. 1653–1656, 2006.
- [35] G. Mie, "Beiträge zur Optik rüber Medien, speziell kolloidaler Metallösungen," *Annalen der Physik*, vol. 330, pp. 377–445, 1908, *Drude's Ann.*, Vol. 25, pp. 377–445, 1908.
- [36] J. C. Seferis, "Refractive indices of Polymers," in *Polymer Handbook*, J. Brandrup and E. H. Immergut, Eds., pp. VI/451–VI/461, Wiley, New York, NY, USA, 1989.



Hindawi

Submit your manuscripts at
<http://www.hindawi.com>

